Supershell structure of magnetic susceptibility

S. Frauendorf
Institute for Nuclear and Hadronic Physics, Research Center Rossendorf, PB 51 01 19, D-01314 Dresden, Germany

V. M. Kolomietz, A. G. Magner, and A. I. Sanzhur
Institute for Nuclear Research, 252028 Prospekt Nauki 47, Kiev–28, Ukraine

(Received 24 March 1998)

The magnetic susceptibility of electrons confined to a spherical cavity or a circular billiard shows slow oscillations as a function of the number of electrons, which are a manifestation of the supershell structure found in the free energy of metal clusters. The relationship of the oscillations of the two different quantities is analyzed by means of semiclassical calculations, which are in quantitative agreement with quantal results. The oscillations should be observable for ensembles of circular ballistic quantum dots and metal clusters.
[S0163-1829(98)03533-4]

I. INTRODUCTION

The confinement of independent fermions in two or three dimensions (3D) leads to a bunching of the single particle levels, if the mean free path of the fermions is large compared to the size of the system. This is known as shell structure (SS) and leads to oscillations of the total energy as function of particle number N around a smoothly changing background. The oscillating part, referred to as shell energy, has minima at the so-called magic numbers, which have been known for a long time for nuclei. More recently they have been observed in the abundance spectra of alkali metal clusters (see Ref. 1 and the original work cited therein), representing minima of the free energy.[2] Later, it was found,[3] that the amplitude of these shell oscillations is modulated by a slow oscillation. This so-called supershell structure (SSS) had been predicted theoretically.[4,5] In this paper we will show that the magnetic susceptibility follows a similar SSS pattern. Using the Strutinsky shell correction method[6–8] and semiclassical periodic orbit theory (POT), we will trace the SSS of the susceptibility and free energy back to the same interference pattern between electrons on classical periodic orbits.

The consequences of SS for the magnetic susceptibility of the confined electron gas have been discussed in Refs. 9–13, and earlier references cited therein. The susceptibility of a confined ballistic 2D electron gas can be measured for large ensemble of quantum dots on a AlGaAs-GaAs semiconductor heterostructure.[9] For this type of experiment it is claimed[9,11–13] that the shell oscillations as a function of the electron number N are averaged out by the fluctuations of the size and the shape of the individual dots. The only quantum size effect (QSE's) expected to survive is a paramagnetic enhancement of the susceptibility, which changes smoothly with N. In this paper we will argue that such experiments should permit us to resolve the slow oscillations reflecting the SSS. We will also discuss the experimental possibilities to detect SSS of the magnetic susceptibility of metallic clusters.

II. SUSCEPTIBILITY OF ELECTRONS IN A SPHERICAL CAVITY

Choosing z as the direction of the magnetic field H, the orbital part of the electronic Hamiltonian is[15]

$$\mathcal{H}=\mathcal{H}_0+\omega L_z+\frac{M\omega^2}{2}(x^2+y^2), \tag{1}$$

where $\mathcal{H}_0$ is the Hamiltonian at zero magnetic field, consisting of kinetic energy and the confining potential, which is assumed to be circular or spherical. The operator L_z is the angular momentum projection on the z axis and M the effective electron mass. We use the Larmor frequency $\omega=\mu_B H/\hbar$ as the unit of the magnetic field H in order to stress the analogy to the case of a system rotating with the angular velocity $-\omega$.

Up to third order of perturbation theory in ω, the thermodynamical potential $\Omega(T,\lambda,\omega)$ as a function of the temperature T and chemical potential λ is

$$\Omega(T,\lambda,\omega)=-T\sum_\nu \ln\left[1+\exp\left(\frac{\lambda-\varepsilon_\nu-\hbar\omega m_\nu-M\omega^2\langle x^2+y^2\rangle_\nu/2}{T}\right)\right], \tag{2}$$

where ε_ν, m_ν, and $\langle\cdots\rangle_\nu$ are the energy, the angular momentum projection, and the expectation value with the unperturbed electron state ν. In our units, the zero field susceptibility is a moment of inertia. For the grand canonical ensemble it reads

$$\theta=-\left(\frac{\partial^2\Omega}{\partial\omega^2}\right)_{\omega=0}=\theta_{\rm cr}-\theta_{\rm rig}, \tag{3}$$

$$\theta_{\rm cr}=\sum_\nu (\hbar m_\nu)^2\frac{\partial n_\nu}{\partial\lambda}, \tag{4}$$

$$\theta_{\rm rig}=M\int d\mathbf{r}\rho(\mathbf{r})(x^2+y^2), \tag{5}$$

where $n_\nu=\{1+\exp[(\varepsilon_\nu-\lambda)/T]\}^{-1}$ are the Fermi occupation numbers and $\theta_{\rm rig}$ is the moment of inertia of rigid rotation, $\rho(\mathbf{r})$ being the particle density.

The shell structure of $\theta_{\rm cr}$ has been analyzed for nuclear rotation (where it is called the cranking moment of inertia). Following the concepts of Strutinsky's shell correction method,[6,7] Ω, $\theta_{\rm cr}$, and other quantities are divided into a smooth part and into a shell part (denoted by the subscript sh). The shell contribution to $\theta_{\rm cr}$, which we call $\theta_{\rm sh}$, represents the total QSE, because the shell part of $\theta_{\rm rig}$ is negligible as compared to $\theta_{\rm sh}$. The partition can either be done numerically starting from the quantal electron levels[6–8] or it can be based on semiclassical periodic orbit theory (POT). In the latter case the shell terms read[16,17,13]

$$\begin{Bmatrix}\theta_{\rm sh}(T,\lambda)\\ \Omega_{\rm sh}(T,\lambda)\end{Bmatrix}=2\sum_\beta \begin{Bmatrix}a(\ell_\beta)^2\\ (\hbar/\tau_\beta)^2\end{Bmatrix}A_\beta(\lambda) \times\sin\left(\frac{1}{\hbar}S_\beta(\lambda)+\nu_\beta\right)\frac{T\tau_\beta/\hbar}{\sinh(T\tau_\beta/\hbar)}, \tag{6}$$

where $\Omega_{\rm sh}$ denotes the value at zero field and $a=1$ or $\frac{1}{3}$ in 2D or 3D, respectively. For the spherical cavity[4] and the circular billiard[12,13] the orbits $\beta(t,p)$ are defined by the number t of the revolutions around the center and the number p of the corners,

$$L_\beta=2pR\sin\phi,\quad \phi=\pi t/p, \tag{7}$$

$$S_\beta=\hbar kL_\beta,\quad \ell_\beta=\hbar kR\cos\phi,\quad \tau_\beta=\frac{ML_\beta}{\hbar k}, \tag{8}$$

$$A_\beta=\frac{2MR^2}{\hbar^2}\frac{1}{\sqrt{kR}}\frac{f_\beta(\sin\phi)^{3/2}}{\sqrt{p\pi}}(p\geqslant 2t),\quad \text{2D}, \tag{9}$$

$$A_\beta=\frac{2MR^2}{\hbar^2}\sqrt{kR}\sin(2\phi)\sqrt{\frac{\sin\phi}{p\pi}}(p>2t),\quad \text{3D}, \tag{10}$$

$$A_d=\frac{2MR^2}{\hbar^2}\frac{1}{p\pi}(p=2t),\quad \text{3D}, \tag{11}$$

$$\nu_\beta=-\frac{3\pi}{2}p+\frac{3\pi}{4},\quad \text{2D}, \tag{12}$$

$$\nu_\beta=-\frac{3\pi}{2}p-(t-1)\pi-\frac{\pi}{4},\quad \text{3D}, \tag{13}$$

where we have introduced the length of the orbit L_β, the wave number $k=\sqrt{2M\lambda/\hbar^2}$, and $f_\beta=1$ for diameters and 2 for planar orbits. The phases ν_β, which are related to the Maslov indices, are not important in our discussion and are given in Refs. 4 and 13. The POT level densities of a spherical cavity and a circular billiard in a magnetic field have been studied in Refs. 18 and 19.

Since the energy to extract one electron from the confining potential is much higher than the temperature, it is important to use the canonical ensemble and define the susceptibility as the derivative $\theta=-(\partial^2F/\partial\omega^2)_{\omega=0}$ of the free energy at fixed particle number N. The importance of the fixed electron number for the magnetic properties of 2D structures has been pointed out previously.[12,13] We adopt the approximation valid for large N, calculating $F(T,N,\omega)=\Omega(T,\lambda,\omega)+\lambda N$, where λ is found from the condition

$$-\partial\Omega(T,\lambda,\omega)/\partial\lambda=N. \tag{14}$$

The zero field susceptibility is given by expressions (3) or (6) taken at $\lambda(N)$ fixed by Eq. (14) at $\omega=0$. We solve this equation numerically both for the semiclassical and the quantum calculation.

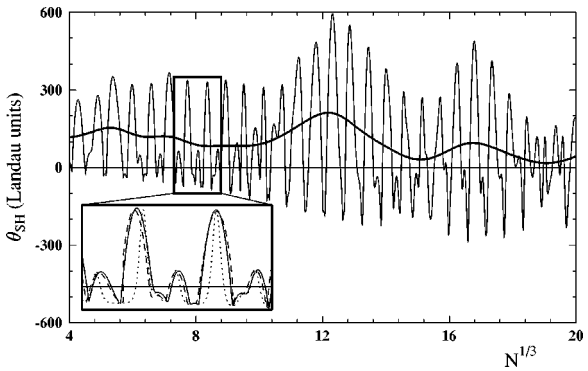

FIG. 1. Shell contribution $\theta_{\rm sh}$ of the magnetic susceptibility of N electrons in a spherical cavity. The effective mass is $M=M_e$, the radius $R=r_sN^{1/3}$ with $r_s=0.208$ nm, the Fermi energy $\varepsilon_F=3.24$ eV, and the temperature $T=0.005\varepsilon_F=170$ K. The thin line shows the results without averaging over $N^{1/3}$ and the fat ones after averaging with a Gaussian of width $\Delta N^{1/3}=0.75$. Inset: solid and dashed lines show the quantum and semiclassical calculations for the canonical ensemble, respectively. Dots present the grand canonical quantum result (fixed $\lambda=\varepsilon_F$).

III. SPHERICAL CAVITY

Figure 1 shows $\theta_{\rm sh}(N,T)$ calculated by means of the numerical Strutinsky averaging procedure[8] from the quantal levels in a spherical cavity. The parameters are appropriate for sodium. As a unit we use the Landau diamagnetic susceptibility (LU) for the electron gas in the cavity $|\theta_L|=0.2715MNr_S^2$. Since all contributions to the bulk susceptibility are of the same order of magnitude,[15] the figure directly shows the enhancement due to the QSE.

The susceptibility $\theta_{\rm sh}$ oscillates with the period of the shells. In addition its amplitude is modulated with a slow oscillation, which is the supershell structure first noticed for the level density.[4,5] It was found experimentally in the abundances of Na clusters,[3] which are determined by $F_{\rm sh}{}^2$, showing also the SSS pattern (cf. Fig. 2).

We have also evaluated $\theta_{\rm sh}$ by means of the POT sums (6). As seen in the inset of Fig. 1, the quantal values of $\theta_{\rm sh}$ agree very well with ones obtained from the semiclassical expression. Semiclassics permits a simple interpretation of the SSS. The shortest PO's enclosing magnetic flux are the triangle and square. The temperature factor $1/\sinh(T\tau_\beta/\hbar)\approx 2\exp(-L_\beta/\Lambda_T)$, where $\Lambda_T=\hbar^2k/TM$ is the characteristic ''temperature length,'' dampens the longer orbits. The beat

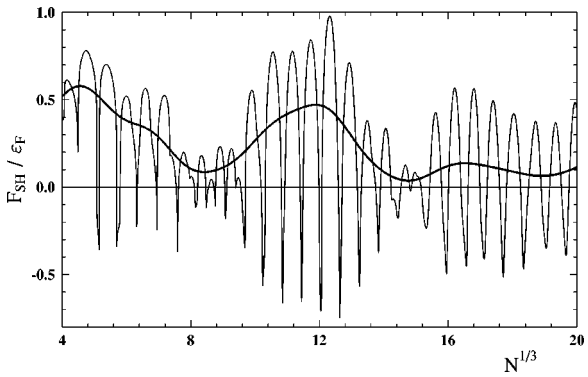

FIG. 2. Shell contribution $F_{\rm sh}$ to the free energy of N electrons in a spherical cavity. The calculation and the conventions are identical to those in Fig. 1.

pattern results from the superposition of the two leading terms, the triangle and the square. The basic oscillation has a period given by $k(L_{\triangle}+L_{\square})/2$ and the beat oscillates with $k(L_{\square}-L_{\triangle})$. Figure 3 shows a calculation that takes into account only the triangle and the square. Comparing with the full calculation, the influence of the longer orbits is seen. Although they make the peaks higher the beat pattern is not much changed up to $N^{1/3}\sim 16$. The upper and lower envelops of the full calculation are not very different from the ones of the truncated calculation. This demonstrates that the beat pattern is basically generated by the triangle and the square. For $N^{1/3}\gtrsim 16$, the full calculation has a beat minimum where the truncated one has a maximum, indicating that the interference with the longer orbits becomes important.

IV. RELATION TO THE SHELL STRUCTURE IN THE FREE ENERGY

The relation between the shell contributions to the zero field free energy, $F_{\rm sh}$ and to the susceptibility $\theta_{\rm sh}$ is understood by comparing the two POT sums (6). The terms are identical up to the factor

$$\Upsilon_{\beta}=a(l_{\beta}\tau_{\beta}/\hbar)^2=\hbar^{-2}M^2R^4ap^2\sin^2(2\phi) \qquad (15)$$

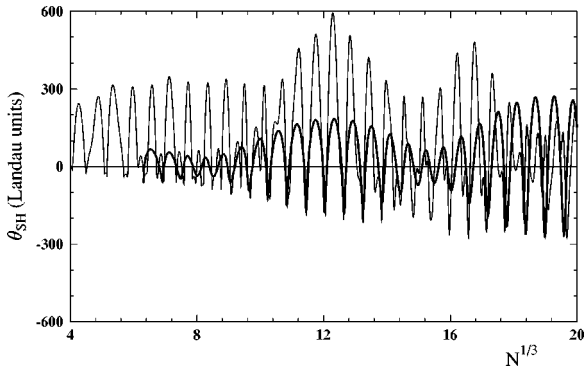

FIG. 3. Shell contribution $\theta_{\rm sh}$ of the magnetic susceptibility of N electrons in a spherical cavity. The thin line is the same as in Fig. 1, the thick line corresponds to a calculation where only the triangular and square orbits in the POT sums (6) are taken into account. For $N^{1/3}<6$ the level density is not positive definite in this approximation and the solution of Eq. (14) is not possible.

in $\theta_{\rm sh}$, which suppresses the orbits $l_{\beta}=0$ and gives the long orbits a higher weight. If only few orbits with similar values of $\Upsilon_{\beta}\approx\Upsilon$ contribute, $\theta_{\rm sh}\approx\Upsilon F_{\rm sh}$. The simple scaling is also expected to hold for shapes not too different from the sphere and can be used to relate the SS in the susceptibility and free energy.

In the 3D case the diameter orbit is suppressed by a factor $1/\sqrt{kR}$ as compared to the planar orbits, because it has a lower degeneracy. This makes its contribution to $F_{\rm sh}$ insignificant for large N. The two sums $F_{\rm sh}$ and $\theta_{\rm rs}$ become similar, because the leading terms are the triangle and square. In fact, for $T>0.02\varepsilon_F$ we find $\theta_{\rm sh}\approx\Upsilon F_{\rm sh}$ with $p=3-4$ in Eq. (15) (where ε_F is the Fermi Gas energy). For the lower temperature $T=0.005\varepsilon_F$, shown in Figs. 1 and 2, we find a ratio Υ with $p=4$ at the SSS maxima ($N^{1/3}=12$ and 17). The SSS minima are less pronounced for $\theta_{\rm sh}$ than for $F_{\rm sh}$. There the triangle and square cancel each other. The main contribution comes from longer orbits, which are much more important for $\theta_{\rm sh}$ than for $F_{\rm sh}$, preventing $\theta_{\rm sh}$ from becoming as small as $F_{\rm sh}$. This interpretation is also supported by Fig. 3. The difference between the full and truncated calculations, which represents the contribution of the longer orbits, is just an up shift of the upper envelope.

The SSS is clearly developed for the temperature of $T=0.005\varepsilon_F$, shown in Fig. 1. For $T=0.0005\varepsilon_F$ we find very pronounced SS with an amplitude of a few thousand LU, but little SSS. The averaged susceptibility stays around 1500 LU with small peaks (400 LU high) at $N^{1/3}=7$ and 13. Due to a weak temperature damping in the POT sum many orbits contribute to the sum, destroying the simple beat pattern. This is at variance with a distinct SSS pattern in $F_{\rm sh}$ persisting to $T=0$.[4,5] The reason is the factor $1/\Upsilon_{\beta}$ which suppresses the orbits with high p. For $T=0.05\varepsilon_F$ there is SSS, but the amplitude of the basic shell oscillations remains below 5 LU for $N<100$, becoming small compared with the LU for larger N. Hence, the intermediate temperature seems to be optimal for the observation of the SSS.

V. CANONICAL ENSEMBLE

Experimentally, the average susceptibility of an ensemble of clusters with a distribution in N will be measured. Let us consider a Gaussian distribution in $N^{1/3}$ of width $\Delta(N^{1/3})=0.75$, which corresponds to about one oscillation. As shown in Fig. 1, averaging the susceptibility damps out only the basic shell oscillations, whereas the SSS remains as a modulation of the strongly paramagnetic susceptibility. Hence, it is expected that the SSS can be observed with a moderate mass selection of the clusters that would not allow us to resolve the basic SS ($\Delta N/N=0.23$ for $N=1000$ in Fig. 1).

The QSE of the susceptibility survives the averaging only for the canonical ensemble.[9,11–13] The inset of Fig. 1 compares the canonical with grand canonical ensemble ($\lambda=\varepsilon_F$). Though the positions of the extrema are similar, the shape of peaks is rather different. For the grand canonical ensemble the negative and positive values are equally probable and, as the result, averaging with respect to N quenches $\theta_{\rm sh}$. For the canonical ensemble, the positive values are more frequent and the QSE survives the averaging with respect to N. The preference of $\theta_{\rm sh}>0$ for the canonical ensemble is evident

from POT sum (6): The shell correction to the level density $g_{\rm sh}$, which is given by setting the factor $\{\cdots\}=1$, oscillates in phase with $\theta_{\rm sh}$, i.e., more N values correspond to a paramagnetic than to a diamagnetic susceptibility and the average with respect to the particle number is positive.

Let us discuss this correlation in more detail because it is crucial for the measurability of the SSS. Figure 3 illustrates that typical inverted parabolas already appears for the lowest orbits. It is sufficient to consider only one term in Eq. (6), say the triangle. For the grand canonical ensemble, the wave number $k=k_F$ is constant (k_F is the Fermi gas value). The orbit length is $L_\triangle \propto N^{1/3}$. The susceptibility is proportional to $\sin(k_F L_\triangle)$ (for simplicity the phase $\nu_\triangle$ is left away), which averages to zero. The particle number expectation value as given by (14) contains a term proportional to $-\cos(k_F L_\triangle)$ that makes it oscillating around N. Thus, for the canonical ensemble, the wave number $k=k_F+\delta k$ cannot be constant. It must contain an oscillating term δk in order to satisfy Eq. (14). In order to understand qualitatively its consequences for the susceptibility we use an argument from Refs. 12 and 13. Retaining only the linear order of δk, Eq. (14) gives $\delta k \propto \cos(k_F L_\triangle)$. The susceptibility is proportional to $\sin[(k_F+\delta k)L_\triangle] \approx \sin(k_F L_\triangle)+\delta k L_\triangle \cos(k_F L_\triangle)$. The second term is proportional to $\cos(k_F L_\triangle)^2$ which averages to 1/2. Hence, the total averaged susceptibility is positive. Since the interference between the triangular and quadratic orbits in both $\theta_{\rm sh}$ and $g_{\rm sh}$ is about the same, the SSS modulates paramagnetic term also after averaging. The oscillations of δk narrow the minima and broaden the maxima of the susceptibility. In our calculations, δk is treated exactly. As seen in Figs. 1 and 3, due to the higher orders in δk the minima are narrowed to cusps and the maxima take the shape of parabolas.

VI. REAL CLUSTERS

Real clusters deviate from the perfect spherical cavity: The surface has a finite thickness of the order of the screening length. The discrete ionic back ground implies a certain surface roughness of the order of the interatomic distance. There may be impurities or other imperfections distributed over the volume.

The SS in a spherical potential with a realistic surface thickness (the one of sodium) has been studied in Ref. 5. The SSS in the binding energies is clearly developed. The beat minima are somewhat shifted as compared to the cavity. The shift has been be traced back to small changes of the action of the POT due to the modified ''reflection'' by the finite potential at the surface. Since the expressions (6) hold also for the more realistic potentials if the appropriate action S is inserted, a similar shift of the SSS pattern can be inferred for the susceptibility.

The consequences of the surface roughness for the shell structure of the ground state energy have been studied in Ref. 21. The energy is given by the POT sum (6), where each term contains an additional damping factor χ^p. Assuming that the rough surface is randomly displaced relative to the ideal one, the damping factor is

$$\chi^p = \exp[-2p(\sigma k \sin\phi)^2], \tag{16}$$

where a Gaussian displacement distribution with the width $\sigma \sim r_S$ is used. It has a simple interpretation. The number of reflection on the surface is p. For each reflection the rough surface scatters a certain fraction of the particles away from the POT. The arguments of Ref. 21 can be immediately taken over to the zero field susceptibility. The damping factor arises from the reflections on the irregular surface. A weak magnetic field does not change the reflections on the surface (the difference between the case with a weak and without a field is the small curvature of the trajectory between the reflection points which barely changes the angles of the trajectory with the surface) and the damping factor (16) also appears in the susceptibility. Hence, the long orbits (large number of reflections p) are strongly suppressed by the surface roughness. In Ref. 21 it is shown that a roughness $\sigma=0.2r_S=0.38/k_F$ reduces the amplitude of the SS to about 1/2 of the one of the ideal cavity. The SSS is found to be nearly the same as for the ideal cavity. For the susceptibility one expects that the surface roughness strongly reduces the contributions of the long orbits, such that the SSS pattern of Fig. 1 approaches the one of Fig. 3 with a reduced amplitude. In particular, for very low temperature the surface roughness is expected to enhance the SSS, because it efficiently damps the long orbits.

Impurities or other imperfections that are homogeneously distributed over the volume will also scatter the particles away from the POT. The situation is analogous to the propagation of a wave in an absorbing medium, which has been considered in Ref. 4. The scattering results in a damping factor of the form $\exp(-L_\beta/\Lambda_I)$, where $1/\Lambda_I$ measures the amount of scattering per unit length and corresponds to the mean free path of the electrons due to the imperfections. This kind of damping is equivalent with an increase of the temperature, because the temperature damping factor in Eq. (6) $1/2\sinh(T\tau_\beta/\hbar) \approx \exp(-L_\beta/\Lambda_T)$. The consequences of a temperature increase are discussed above.

VII. MEASUREMENTS OF THE SUSCEPTIBILITY OF METAL CLUSTERS

In Ref. 14 the susceptibility has been measured for three ensembles of clusters with average sizes of $N^{1/3} \approx 4$, 2, and 1.5 and a large spread in size. A paramagnetic enhancement of 5, 2, and 1.5 is found, respectively. The decrease of the enhancement with N, which Ref. 14 refers to as an unexplained phenomenon, can be seen in Fig. 1. To identify the SSS, experiments with more points in N and a mass resolution better than 30% are needed. An alternative experiment would be the measurement of the deflection of a cold cluster beam in an inhomogeneous magnetic field, which directly provides the susceptibility. To reach the necessary sensitivity of such a Stern-Gerlach apparatus seems to be possible.[22] It is favorable for this kind of experiment that only a moderate mass selection is needed to observe SSS, which permits larger intensities.

Measuring the susceptibility could shed new light on the electronic structure of small metal clusters. Solid icosahedral shapes have been suggested for sodium clusters with $T \sim 200$ K.[23] Our sphere model should be a rough first approximation for $N<1000$. In this range the shell energies $E_{\rm sh}$ for the spherical and icosahedral cavity are similar[24] and, as dis-

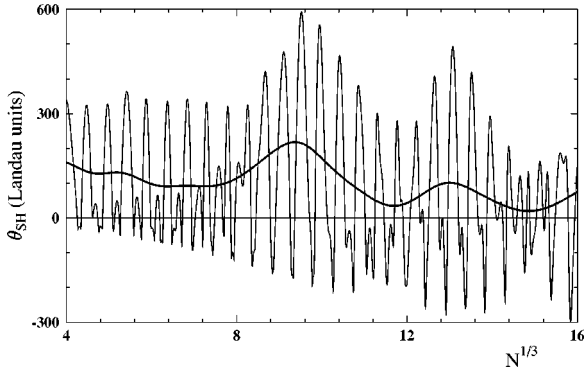

FIG. 4. Shell contribution of the magnetic susceptibility N electrons in a half spherical cavity. The line conventions and calculation [except $R=r_S(N/2)^{1/3}$] are identical to those in Fig. 1.

cussed above, the same can be expected for the susceptibilities. A more pronounced paramagnetic SSS is expected if the shape of the cold clusters comes close to a rough sphere. The picture changes if the clusters are liquid or if they keep the same shape as in the liquid state when freezing at low T. Then magic clusters are spherical and strongly diamagnetic, whereas the nonmagical ones are deformed and weakly diamagnetic.[20] Thus, the averaged susceptibility would be diamagnetic, still showing a SSS.

VIII. HALF SPHERE

Figure 4 shows the susceptibility for a half sphere with $R=r_S(N/2)^{1/3}$. The results are very similar to the full sphere. The main difference is a shift of the basic shell oscillations by half a period. The averaged susceptibility is almost indistinguishable from Fig. 1. Clusters deposited on an insulating surface may take shapes close to half spheres.[25–27]

IX. CIRCULAR QUANTUM DOTS

The susceptibility of the 2D electron gas confined to a circular potential well with $R=500$ nm is shown in Fig. 5. An effective mass of $M=0.067M_e$,[28] appropriate for GaAs,

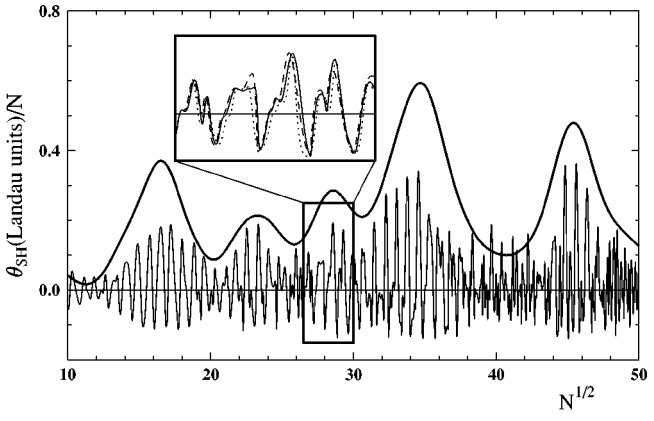

FIG. 5. Shell contribution $\theta_{\rm sh}$ to the magnetic susceptibility of N electrons in a circular well. The effective mass is $M=0.067M_e$, the well radius $R=500$ nm, and the temperature $T=5\hbar^2/2MR^2\approx 0.13$ K. The line conventions are the same as in Fig. 1. Averaging over $N^{1/2}$ is carried out with a Gaussian of width $\Delta N^{1/2}=1.6$. The nonaveraged values are divided by a factor of 10.

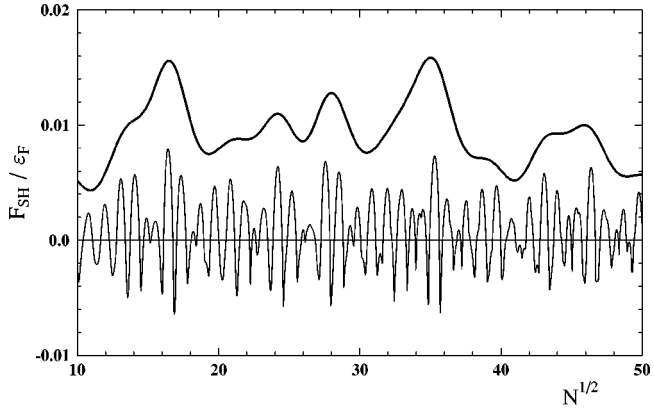

FIG. 6. Shell contribution $F_{\rm sh}$ to the free energy of N electrons in a circular well in units of $\varepsilon_F=N\hbar^2/MR^2$. The calculation and the conventions are identical to those in Fig. 3.

is assumed. The LU is $|\theta_L|=MR^2/3$. The 2D case is similar to the 3D case, the main difference consisting in an increase of the QSE with N (the values in Fig. 5 are divided by N). At the temperature $T=5\hbar^2/2MR^2\approx 0.13$ K a distinct SSS is seen. For $T=0.5\hbar^2/2MR^2$ the averaged susceptibility $\sim 4/N$ LU showing shallow oscillations with an amplitude of $\sim 1/N$ LU, which loosely correlates with the SSS in Fig. 5. A SSS beat pattern for a circular dot has been calculated in Ref. 13. However, it is argued there and also in Refs. 11,12 that when averaging over the ensemble of dots used as experimental probe, uncertainties in the shape and size will completely wipe out the shell structure, the only remaining QSE being a paramagnetic enhancement that varies smoothly with N. In contrast, Fig. 5 shows that averaging with a Gaussian of width $\Delta N^{1/2}=1.6$ (corresponding to a 10% spread in N for $N=1000$) destroys only the basic SS, whereas the SSS remains visible.

Nowadays it is possible to manufacture probes with a large number of circular quantum dots, specifying the radius and the gate voltage with a 5% accuracy.[28] Changing the number of electrons in the dots by means of the gate voltage seems to be a possibility to measure the SSS of the susceptibility. The imperfections in manufacturing circular dots will have similar effects as discussed above for the metal clusters. The discussion of the 3D case can be directly applied to the 2D case. Thus, the SSS pattern is expected to survive if the surface roughness $\sigma<0.4/k_F$.

Figure 6 demonstrates that, in contrast to the 3D case, $F_{\rm sh}(N)$ significantly differs from $\theta_{\rm sh}(N)$. For the 2D case, the diameter orbit is not suppressed in $F_{\rm sh}$. The interference of the diameter, triangle, and square results in slower basic and faster beat oscillations as compared to $\theta_{,\rm sh}$, for which the diameter is missing. Averaging with respect to $N^{1/2}$ filters out the slow oscillation due to the interference between triangle and square, which mainly modulates $F_{\rm sh}(N)$. The SS of the free energy should show up as a modulation of the capacitance of the dot. It is given by d^2F/dN^2, which also determines the abundances of heavy clusters.[2]

X. CONCLUSIONS

The susceptibility of electrons confined in two or three dimensions by a spherical potential oscillates as a function of

their number. This shell structure is modulated by slow oscillations, the supershell structure, which only develops at sufficiently high temperatures. Measurements that average out the shell structure may still reveal the supershell structure. The free energy of electrons confined in three dimensions, shows the analogous supershell pattern, which is observed in the abundances of metal clusters. However, for the two-dimensional potential the shell structure of the free energy differs considerably from the one of the susceptibility.

ACKNOWLEDGMENTS

Discussions with M. Brack and F. A. Ivanyuk and financial support by INTAS (Grant No. 93-0151) are gratefully acknowledged.

[1] W. DeHeer, Rev. Mod. Phys. **65**, 611 (1991).
[2] F. Chandezon, S. Bjørnholm, J. Borggreen, and K. Hansen, Phys. Rev. B **55**, 5485 (1997).
[3] J. Pedersen, S. Bjørnholm, J. Borggreen, K. Hansen, T. P. Martin, and H. D. Rasmussen, Nature (London) **353**, 733 (1991).
[4] R. B. Balian and C. Bloch, Ann. Phys. (N.Y.) **69**, 76 (1972); **85**, 514 (1974).
[5] H. Nishioka, K. Haansen, and B. R. Mottelson, Phys. Rev. B **42**, 9377 (1990).
[6] V. M. Strutinsky, Nucl. Phys. A **95**, 420 (1967).
[7] V. M. Strutinsky, Nucl. Phys. A **122**, 1 (1968).
[8] V. V. Pashkevich and S. Frauendorf, Sov. J. Nucl. Phys. **20**, 688 (1974).
[9] L. P. Lévy, D. H. Reich, L. Pfeiffer, and K. West, Physica B **189**, 204 (1993).
[10] J. M. van Ruitenbeck and D. A. van Leeuwen, Phys. Rev. Lett. **67**, 640 (1991).
[11] F. v. Oppen, Phys. Rev. B **50**, 17 151 (1994).
[12] D. Ullmo, K. Richter, and R. A. Jalabert, Phys. Rev. Lett. **74**, 383 (1995).
[13] K. Richter, D. Ullmo, and R. A. Jalabert, Phys. Rep. **276**, 1 (1996).
[14] K. Kimura and S. Bandow, Phys. Rev. Lett. **58**, 1359 (1987).
[15] C. Kittel, *Introduction to Solid State Physics* (Wiley, New York, 1978).
[16] V. M. Kolomietz, A. G. Magner, and V. M. Strutinsky, Sov. J. Nucl. Phys. **29**, 758 (1979).
[17] A. G. Magner, V. M. Kolomietz, and V. M. Strutinsky, Sov. J. Nucl. Phys. **28**, 764 (1978).
[18] S. M. Reimann, M. Persson, P. E. Lindelof, and M. Brack, Z. Phys. B **101**, 377 (1996).
[19] K. Tanaka, S. C. Creagh, and M. Brack, Phys. Rev. B **53**, 16 050 (1996).
[20] S. Frauendorf, V. V. Pashkevich, and S. M. Reimann, Surf. Rev. Lett. **3**, 441 (1996).
[21] N. Pavloff, J. Phys. A **28**, 4123 (1995).
[22] S. Federico and W. deHeer (private communication).
[23] H. Göhlich, T. Lange, T. Bergmann, and T. P. Martin, Phys. Rev. Lett. **65**, 748 (1991).
[24] N. Pavloff and S. C. Creagh, Phys. Rev. B **48**, 18 164 (1993).
[25] Y. Z. Li, R. Reifenberger, E. Choi, and R. P. Andres, Surf. Sci. **250**, 1 (1991).
[26] W. Mahoney, D. M. Schaefer, A. Patil, R. P. Andreas, and R. Reifenberger, Surf. Sci. **316**, 383 (1994).
[27] O. Rattunde, Diploma thesis, University of Freiburg.
[28] D. Weiss, Ph.D. thesis, TU München, 1987; (private communication).